

## Preparation of Nanocrystalline $\text{WO}_3$ and $\text{MoO}_3$ by Different Sol–Gel Methods

Y. DIMITRIEV<sup>1</sup>, R. IORDANOVA<sup>2</sup>, M. MANCHEVA<sup>2</sup> and D. KLISSURSKI<sup>2</sup>

<sup>1</sup>University of Chemical Technology and Metallurgy,  
Kl. Ohridski bl. 8, Sofia 1756 (Bulgaria)

<sup>2</sup>Institute of General and Inorganic Chemistry, Bulgarian Academy of Sciences,  
G. Bonchev str., bl. 11, Sofia 1113 (Bulgaria)

E-mail: reni\_11@abv.bg

### Abstract

Two sol–gel methods for the preparation of  $\text{WO}_3$  and  $\text{MoO}_3$  nanopowders were used in this work: i) an ion-exchange reaction and ii) an oxidizing reaction ( $\text{M} + \text{H}_2\text{O}_2$ ). The phase and structural transformations undergone by colloidal solutions of tungsten acid (i) and peroxotungsten and peroxomolybdic acids (ii) as a function of thermal treatment were investigated by X-ray diffraction (XRD) and infrared spectroscopy (IR). Depending on the methods used, different phases were obtained: crystalline hydrates, amorphous and nanocrystalline products. The tungsten trioxide hydrates were prepared by the ion exchange method, crystallization in  $m\text{-WO}_3$  occurring above 300 °C. The tungsten sample being formed in the oxidizing reaction remained amorphous up to 300 °C; above 300 °C,  $m\text{-WO}_3$  crystallized. The particle size of  $m\text{-WO}_3$  was 15 nm irrespective of the methods applied. IR analysis showed that amorphous tungsten network was built by distorted  $\text{WO}_6$  units without participation of peroxo groups ( $\text{O}_2^{2-}$ ). The preparation of  $\text{MoO}_3$  nanopowders by an oxidizing reaction was also studied. Crystallization of  $\text{MoO}_3$  was found to start earlier (200 °C), leading to completely crystallized  $o\text{-MoO}_3$  at 300 °C. The amorphous state of the product was detected at 100 °C only. Comparative analysis of the methods applied showed the oxidizing method to be more suitable for obtaining nanoparticles.

### INTRODUCTION

$\text{WO}_3$  and  $\text{MoO}_3$  are well known metal oxide materials used in gas sensing, catalytic, photochromic and electrochromic research fields. Depending on temperature, there are several crystalline modifications of  $\text{WO}_3$  (triclinic, monoclinic, orthorhombic, tetragonal and hexagonal) [1, 2] while  $\text{MoO}_3$  can exist in two polymorphous forms: orthorhombic and monoclinic [3]. All polymorphs of  $\text{WO}_3$  can be described as distortions from the cubic  $\text{ReO}_3$  structure, which consists of a three-dimensional network of corner-sharing  $\text{WO}_6$  octahedra. The  $\text{ReO}_3$  structure is characteristic of  $m\text{-MoO}_3$  only. The monoclinic  $\text{MoO}_3$  is transformed into orthorhombic  $\text{MoO}_3$  at 400 °C. Crystalline  $o\text{-MoO}_3$  has a layered structure of distorted  $\text{MoO}_6$  polyhedra sharing both edges and corners. One oxygen in each polyhedron is unshared  $\text{M}=\text{O}$  [4]. From the practical point of view, the production of  $\text{MoO}_3$  and  $\text{WO}_3$  nanopowders is interesting. Several

methods have been applied up to now: evaporation [5], sputtering [6] and sol–gel technology [7–14]. There are different sol–gel routes based on different starting compounds: polymerization and polycondensation of metal alkoxides [7], ion exchange methods [8–10] and oxidizing reaction of metallic W or Mo with a solution of  $\text{H}_2\text{O}_2$  [11–13].

The purpose of this study is to obtain  $\text{WO}_3$  and  $\text{MoO}_3$  nanopowders using different sol–gel methods and to compare phase and structure transformations undergone by the precursors.

### EXPERIMENTAL

Two different methods were selected in this study. i) Ion exchange method (A). An aqueous solution of  $\text{Na}_2\text{WO}_4$  was passed through ion-exchange resin to give the sol of tungsten acid [8]. The yellow sol obtained without any organic additives underwent gelation after 30 min at room temperature.

ii) Oxidizing reaction (B) between metal (W or Mo) powder and hydrogen peroxide solution ( $M + H_2O_2$ ) [11]. The sol of peroxotungsten acid was obtained in the presence of ethanol and glacial acetic acid. The peroxotungsten acid was dried at 100 °C to remove the excess of hydrogen peroxide. The obtained sol underwent gelation after 48 h at room temperature.

$MoO_3$  was prepared by oxidizing reaction (B). The sol of peroxomolybdic acid was obtained without organic additives. The obtained sol was transformed into a gel at room temperature too slowly (after two weeks).

The samples obtained were investigated by X-ray phase analysis (APT-15 Philips diffractometer,  $CuK\alpha$  radiation) and infrared spectroscopy in the 1200–400  $cm^{-1}$  region using the KBr pellet technique (Nicolet-320 FTIR spectrometer). The crystallite sizes were calculated using the Scherrer method for the (222) diffraction peak of monoclinic  $m-WO_3$  and (111) diffraction peak of orthorhombic  $o-MoO_3$  powders (the error of crystallite size determination is  $\pm 0.3$  nm).

## RESULTS AND DISCUSSION

### X-ray diffraction analysis

X-ray diffraction patterns of the tungsten sample obtained by the ion exchange method and heated at 100–300 °C are shown in Fig. 1, a. There are principal peaks for  $WO_3 \cdot 2H_2O$  ( $d = 3.67$  Å,  $d = 3.21$  Å,  $d = 2.58$  Å), (18-1419 JCPDS) and for  $WO_3 \cdot 0.33H_2O$  ( $d = 4.90$  Å,  $d = 3.84$  Å,  $d = 3.15$  Å), (35-0270 JCPDS). The ratio between the amorphous and crystalline phases is 1 : 1 (error 10 %). The thermal treatment above 300 °C leads to a visible improvement of the sample crystallinity which is indicated by a strong increase in the intensity of the peaks of  $m-WO_3$  (83-0951 JCPDS) (see Fig. 1, b). The XRD pattern of the sample heated at 400 °C shows a trace of  $WO_3 \cdot 2H_2O$ . Similar results on the presence of hydrated tungsten oxide were obtained using Raman spectroscopy in [10]. The calculated crystallite size of the  $m-WO_3$  powder is 14.5 nm at 400 °C and increases up to 16.7 nm at 600 °C.

The tungsten sample prepared by  $W + H_2O_2$  reaction is amorphous up to 300 °C (Fig. 2). Above

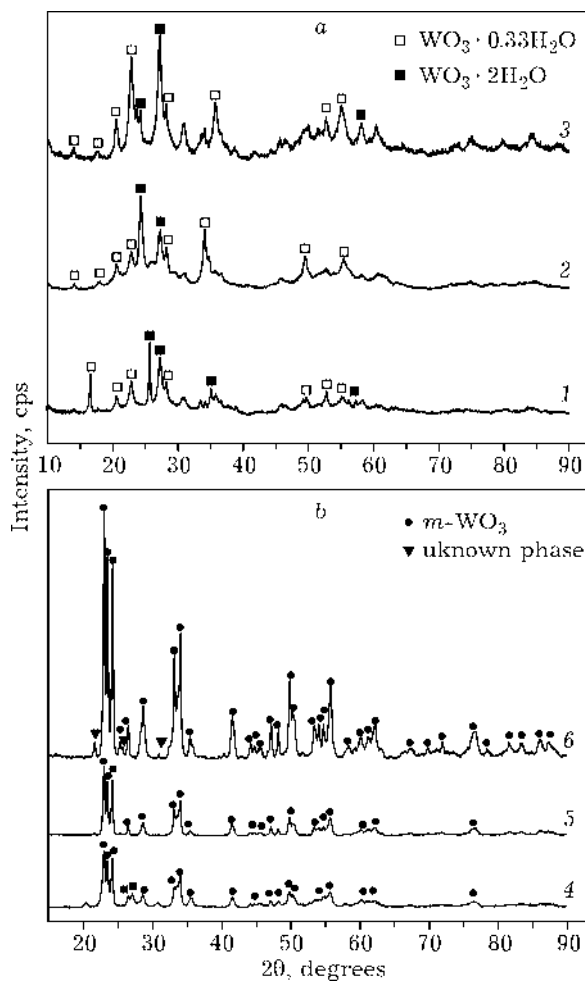


Fig. 1. XRD patterns of the tungsten sample obtained by method A. Temperature, °C: 100 (1), 200 (2), 300 (3), 400 (4), 500 (5), 600 (6).

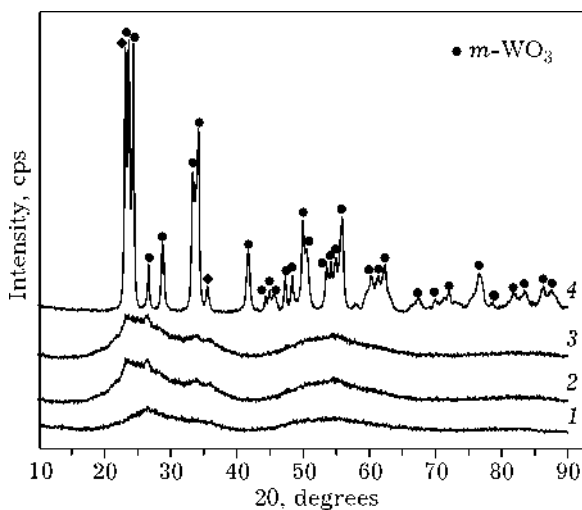


Fig. 2. XRD patterns of the tungsten sample prepared by method B. Temperature, °C: 100 (1), 200 (2), 300 (3), 400 (4).

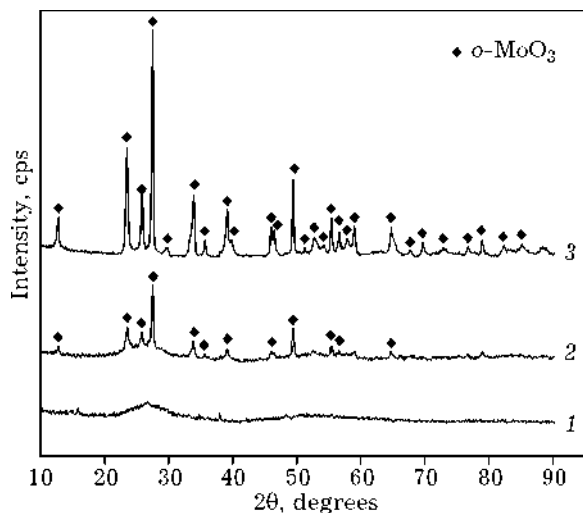


Fig. 3. XRD patterns of the molybdenum sample prepared by method B. Temperature, °C: 100 (1), 200 (2), 300 (3).

300 °C monoclinic  $\text{WO}_3$  (83-0951 JCPDS) appears. The calculated crystallite size of  $m\text{-WO}_3$  powder obtained by this method is 15 nm and does not change with further temperature rise.

The results of these studies show that the amorphous tungsten sample obtained by the oxidizing reaction is kinetically more stable.

Figure 3 presents the XRD patterns of the molybdenum sample obtained by  $\text{Mo} + \text{H}_2\text{O}_2$  reaction and thermal treatment in the temperature range of 100–300 °C. In this case amorphous state is observed at 100 °C only. Further thermal treatment (200 °C) leads to partial crystallization of orthorhombic  $\text{MoO}_3$  (35-0609 JCPDS) which completely crystallizes at 300 °C. The calculated crystallite size of  $o\text{-MoO}_3$  powder is 25.8 nm.

#### Infrared analysis

Figure 4 shows the infrared spectra of the tungsten sample obtained by the ion exchange method. The bands characteristic of tungsten trioxide hydrates are observed in the spectra of the sample heated at 100–300 °C. The bands above 900  $\text{cm}^{-1}$  are assigned to the stretching mode of the terminal  $\text{W}=\text{O}$  bond which is common for all types of  $\text{WO}_3 \cdot n\text{H}_2\text{O}$  [2]. The bands between 800 and 600  $\text{cm}^{-1}$  correspond to  $\nu(\text{W}-\text{O}-\text{W})$  stretching modes. The bands below 600  $\text{cm}^{-1}$  are due to the bending modes of tungsten trioxide [8]. All bands characteristic of crystalline  $m\text{-WO}_3$  are observed in the spectra of

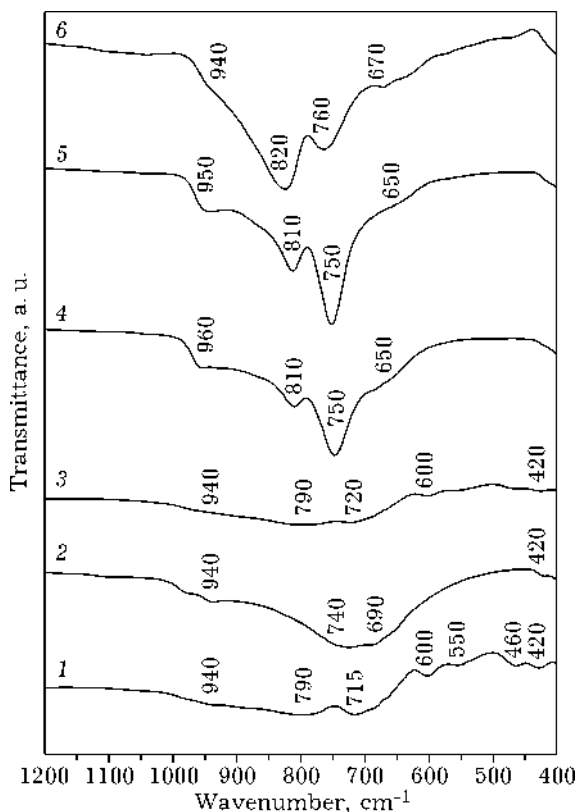


Fig. 4. IR spectra of the tungsten sample obtained by method A. Temperature, °C: 100 (1), 200 (2), 300 (3), 400 (4), 500 (5), 600 (6).

the sample treated above 300 °C. The presence of a high-frequency band at 960 (950)  $\text{cm}^{-1}$  in the spectra of the sample heated at 400 and 500 °C is an indication that the  $\text{WO}_6$  polyhedra building  $m\text{-WO}_3$  are distorted. The transformation of this band into a shoulder as well as the change in the intensity of the bands at 820 and 760  $\text{cm}^{-1}$  in the spectra of the sample treated at 600 °C are probably a result of the formation of more symmetric  $\text{WO}_6$  polyhedra.

The infrared spectra of the tungsten sample obtained by  $\text{W} + \text{H}_2\text{O}_2$  reaction are shown in Fig. 5. The spectra of the sample treated at 100 and 200 °C contain bands characteristic of peroxy complexes: 980  $\text{cm}^{-1}$  ( $\nu\text{W}=\text{O}$ ), 900  $\text{cm}^{-1}$  ( $\nu\text{O}-\text{O}$ ), 810  $\text{cm}^{-1}$  ( $\nu\text{W}-\text{O}-\text{W}$ ) and 560  $\text{cm}^{-1}$  ( $\nu_{\text{as}}\text{W}-\text{O}-\text{O}$ ) [14, 15]. The band at 650  $\text{cm}^{-1}$  has a complex character and may be attributed to  $\nu\text{W}-\text{O}-\text{W}$  and  $\nu_{\text{s}}\text{W}-\text{O}-\text{O}$  vibrations [15, 16]. It should be noted that at low pH of the solution mainly monoperoxy species are formed and a shift of the peroxy bands position to high wave numbers is observed [15]. The band at 560  $\text{cm}^{-1}$  as-

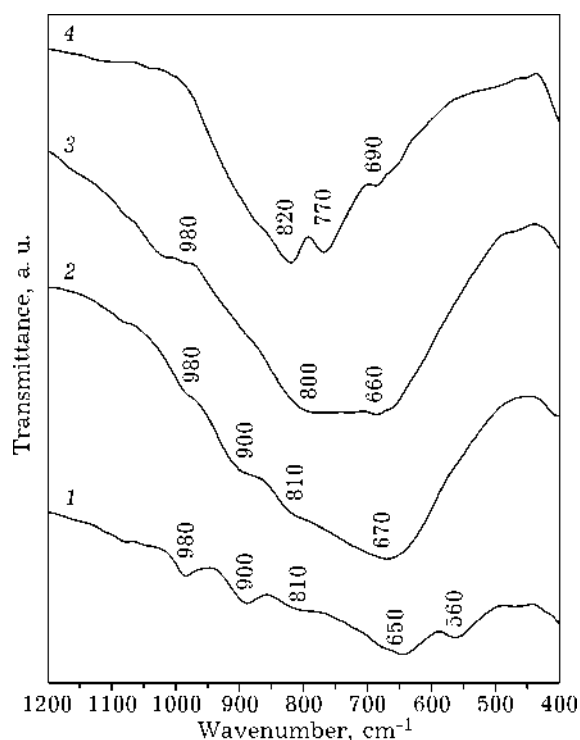


Fig. 5. IR spectra of the tungsten sample prepared by method B. Temperature, °C: 100 (1), 200 (2), 300 (3), 400 (4).

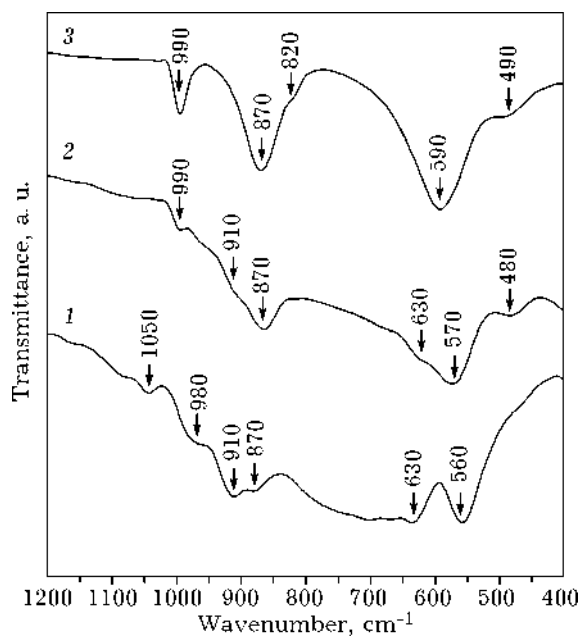


Fig. 6. IR spectra of the molybdenum sample obtained by method B. Temperature, °C: 100 (1), 200 (2), 300 (3).

signed to the vibration of peroxo (W–O–O) groups disappears at 200 °C while the band at 900 cm<sup>-1</sup> attributed to the vibration of (O–O) bond vanishes at 300 °C. The weak band at 980 cm<sup>-1</sup> and bands in the broad absorption region between 800 and 650 cm<sup>-1</sup> in the spectrum at 300 °C can be assigned to stretching vibrations of distorted WO<sub>6</sub>, building the amorphous network [11]. The presence of bands characteristics of WO<sub>6</sub> units is an indication that the number of peroxo groups (O<sub>2</sub><sup>2-</sup>) decreases in the amorphous network formed at 300 °C. Bands typical of crystalline *m*-WO<sub>3</sub> appear in the spectrum of the sample thermally treated at 400 °C.

Figure 6 presents infrared spectra of the sample prepared by the Mo + H<sub>2</sub>O<sub>2</sub> reaction. The spectra of the sample heated at 100 °C show bands characteristic of peroxo complexes: 980 cm<sup>-1</sup> (νMo=O), 910 cm<sup>-1</sup> (νO–O), 870 cm<sup>-1</sup> (νMo–O–Mo), 630 cm<sup>-1</sup> (ν<sub>s</sub>Mo–O–O) and 560 cm<sup>-1</sup> (ν<sub>as</sub>Mo–O–O) [14, 15]. The bands at 910 and 630 cm<sup>-1</sup> characteristic of peroxo groups are transformed into shoulders with increasing temperature (200 °C) and disappear at 300 °C. The infrared spectrum of the sample thermally treated at 300 °C is typical of *o*-MoO<sub>3</sub>.

## CONCLUSIONS

1. Depending on the method and thermal treatment used, it is possible to obtain different tungsten phases: crystal-like hydrates, amorphous or nanocrystalline *m*-WO<sub>3</sub>.
2. The final product at 400 °C is the same (*m*-WO<sub>3</sub>) irrespective of the methods applied. The average crystallite size is 15 nm.
3. With peroxo sol-gel methods, nanocrystalline MoO<sub>3</sub> powder is obtained. The average crystallite size is 25 nm.
4. In comparison with WO<sub>3</sub>, crystallization of MoO<sub>3</sub> starts at a lower temperature (200 °C).
5. It is established that the use of the method B is more appropriate for the preparation of nanocrystalline WO<sub>3</sub> and MoO<sub>3</sub>.

## REFERENCES

- 1 P. Woodward, A. Cleight and T. Vogt, *J. Solid State Chem.*, 131 (1997).

- 2 M. Daniel, B. Desbat, J. Lassegues *et al.*, *Ibid.*, 67 (1987) 235.
- 3 L. Seguin, M. Figlarz, R. Cavagnat and J. Lassegues, *Spectrochim. Acta.*, Part A 51 (1995) 1323.
- 4 L. Kihlborg, *Ark. Kemi*, 24 (1963) 357.
- 5 O. Bohnke, C. Bohnke, G. Robert and B. Carquile, *Solid State Ionics*, 6 (1982) 121.
- 6 M. Green, W. Smith and J. Weiner, *J. Mater. Sci. Lett.*, 38 (1976) 89.
- 7 K. Galatsis, Y. Li, W. Wlodarski and K. Kalantar-Zadeh, *Sens. Actuators*, B77 (2001) 478.
- 8 A. Chemseddine, F. Babonneau and J. Livage, *J. Non-Cryst. Solids*, 9 (1987) 271.
- 9 G. Xu and L. Chen, *Solid State Ionics*, 28-30 (1988) 1726.
- 10 C. Santato, M. Odzienkowski, M. Ulmann and J. Augustynski, *J. Am. Chem. Soc.*, 123 (2001) 10639.
- 11 T. Nanba, S. Takano, I. Yasui and T. Kudo, *J. Solid State Chem.*, 90 (1991) 47.
- 12 U. Krašovec, A. Vuk and B. Orel, *Electrochim. Acta*, 46 (2001) 1921.
- 13 Z. Wang and X. Hu, *Ibid.*, 46 (2001) 1951.
- 14 A. Dengel, W. Griffith, R. Powell and A. Skapski, *J. Chem. Soc. Dalton Trans.*, (1987) 991.
- 15 N. Campbell, A. Dengel, C. Edwards and W. Griffith, *Ibid.*, (1989) 1203.
- 16 B. Pecquenard, S. Castro-Garcia, J. Livage *et al.*, *Chem. Mater.*, 10 (1998) 1882.